Transfer and Transcriptomic Profiling in Liver and Brain of European Eels (*Anguilla anguilla*) After Diet-borne Exposure to Gold Nanoparticles

Perrier Fanny [1], Bertucci Anthony [1], Pierron Fabien [1], Feurtet-Mazel Agnes [1], Simon Olivier [2], Klopp Christophe [3], Candaudap Frederic [4], Pokrovski Oleg [4], Etcheverria Bruno [1], Mornet Stephane [5], Baudrimont Magalie [1, *]

[1] Université de Bordeaux, CNRS, UMR EPOC 5805, Arcachon, France
[2] LECO, IRSN, PSE ENV, SRTE, Cadarache, Saint-Paul-lez-Durance Cedex, France
[3] Plate-forme bio-informatique Genotoul, Mathématiques et Informatique Appliquées de Toulouse, INRA, Castanet-Tolosan, France
[4] Université de Toulouse, CNRS, GET, UMR 5563, Toulouse, France
[5] Université de Bordeaux, CNRS, Bordeaux INP, ICMCB, UMR 5026, Pessac, France Abstract:

* Corresponding author : Magalie Baudrimont, email address : magalie.baudrimont@u-bordeaux.fr

Abstract :

A nanometric revolution is underway, promising technical innovations in a wide range of applications and leading to a potential boost in environmental discharges. The propensity of nanoparticles (NPs) to be transferred throughout trophic chains and to generate toxicity was mainly assessed in primary consumers, whereas a lack of knowledge for higher trophic levels persists. The present study focused on a predatory fish, the European eel (Anguilla anguilla) exposed to gold NPs (AuNPs; 10 nm, polyethylene glycol-coated) for 21 d at 3 concentration levels in food: 0 (NP0), 1 (NP1), and 10 (NP10) mg Au kg(-1). Transfer was assessed by Au quantification in eel tissues, and transcriptomic responses in the liver and brain were revealed by a high-throughput RNA-sequencing approach. Eels fed at NP10 presented an erratic feeding behavior, whereas Au quantification only indicated transfer to intestine and kidney of NP1-exposed eels. Sequencing of RNA was performed in NP0 and NP1 eels. A total of 258 genes and 156 genes were significantly differentially transcribed in response to AuNP trophic exposure in the liver and brain, respectively. Enrichment analysis highlighted modifications in the immune system-related processes in the liver. In addition, results pointed out a shared response of both organs regarding 13 genes, most of them being involved in immune functions. This finding may shed light on the mode of action and toxicity of AuNPs in fish.

Keywords : Gold nanoparticles, Anguilla anguilla, RNA sequencing, Diet-borne exposure, Immunity

INTRODUCTION

Manufactured nanoparticles (NP) emerge as potential environmental contaminants due to a broad and increasing use over the last few years (Jeevanandam et al., 2018; Nowack et al., 2012). NPs are expected to reach aquatic ecosystems through several pathways such as surface runoffs of dry or wet depositions (Baalousha et al., 2016). Quantification of engineered nanomaterials in environmental samples remains challenging for analytical chemistry, and concentrations are often estimated regardless of potential transformations (Caballero-Guzman and Nowack, 2016) leading to an uncertainty in the associated risk assessment. This phenomenon is reinforced by the lack of regulation policy on these materials (Hofmann-Amtenbrink et al., 2015).

In particular, several studies evidenced that NPs exhibit a potential of transfer through experimental aquatic food chains (Cedervall et al., 2012; Croteau et al., 2011; Fouqueray et al., 2012; McTeer et al., 2014; Wang et al., 2016). The main documented biological impacts include DNA damages (Cardoso et al., 2014; Wise et al., 2010), disruptions of some enzyme activities (Chichova et al., 2014; Shrivastava et al., 2014), immunotoxicity (Bettini et al., 2017; Park et al., 2010) and cytotoxicity (Freese et al., 2012; Gliga et al., 2014). In environmental literature, toxicological studies of NPs are scarce and mainly focused on *a priori* effects such as oxidative stress and are mainly restricted to biomarkers (Baudrimont et al., 2018; Huerta-García et al., 2014; Ladhar et al., 2014; Qiu et al., 2015). However, suspected emerging contaminants require a without *a priori* method in order to reveal their potential toxicities and their mechanisms of action. This is even more relevant for NPs that exhibit a wide diversity of organic and inorganic forms

(for a review, see Jeevanandam et al., 2018). Such without *a priori* methods are provided by Next Generation (also referred to as high throughput) sequencing technologies like RNA-sequencing (RNAseq) allow to explore the entire repertoire of transcribed genes and the associated biological processes in response to stress. Regarding aquatic environment, few examples of RNAseq based studies of the transcriptome-wide impact of NPs recently emerged either in animals (Gao et al., 2018; Teles et al., 2019; Zhang et al., 2018) or photosynthetic organisms (Garacci et al., 2019).

Amongst nanoparticles, the gold nanoparticles (AuNP) have induced huge scientific and technological interest due to their standardized synthesis procedures, chemical stability in solution, and unique properties (*i.e.* surface plasmon resonance) (Abdelhalim and Mady, 2012; Kimling et al., 2006). This widespread use of AuNPs made them an emerging pollutant and they are now listed amongst representative manufactured nanomaterials (OECD, 2010). Furthermore, AuNP are considered suitable for biomedical applications, such as drug delivery, due to their reactivity with biological interfaces (Cheng et al., 2014). Several studies showed a propensity of AuNPs to transfer from the environment to food-web and to generate toxic impacts in primary consumers (Ferry et al., 2009; Larguinho et al., 2014). Most studies of AuNP bioaccumulation and toxicity were carried out with bivalves (Volland et al., 2015) exposed to water-borne NPs and studies with teleosts (other than the model species *Danio rerio*) are rare (Ferreira et al., 2016; Teles et al., 2016, 2017).

The present experiment focused on transfer and a whole transcriptome screening after diet-borne exposure to gold nanoparticles in the European eel (*Anguilla anguilla*). This predatory fish presents a complex life cycle and, as euryhaline fish, the ability to adapt to a wide range of aquatic ecosystems. Studies have also emphasized eel sensitivity to

pollutants (Geeraerts and Belpaire, 2010; Pierron et al., 2008) and highlighted the bioindicator potential of this species (Belpaire et al., 2008; de Boer et al., 1994). Few studies however investigated the nanoparticle toxicity in eels but only on cultured cells (Costa et al., 2016, 2015; Srikanth et al., 2015) although this species constitutes a confirmed pollutant bioindicator and a top predator for trophic transfer (Tangaa et al., 2016). Liver and brain tissues were chosen as target organs for the RNA-sequencing analyses, respectively for their involvement in biological functions directly targeted by a trophic contamination for liver, and for the capacity of gold nanoparticles to reach fish brain tissue (Geffroy et al., 2012). Moreover, liver was previously used to study short-term transcriptomic effects of NP in fish (Gao et al., 2018; Teles et al., 2016, 2019). This experimental study aimed to investigate (*i*) the potential transfer to a top predatory fish from AuNP-enriched food and (*ii*) the consecutive transcriptomic changes by means of a RNA-Sequencing approach in the liver and brain tissues after a 21-day trophic exposure. We coupled this with various endpoints (feeding, condition index and organo-somatic indices) to evaluate effects at the organismal level.

MATERIALS AND METHODS

Studied species - Immature yellow eels (*Anguilla anguilla*) of 59.56 ± 2.05 g and 33.80 ± 0.33 cm (mean ± SE, $n = 18$) were caught in the Arcachon Bay area, France, considered as a pristine environment (44°41'24''N, 1°01'27''W) in September 2015. Animals were acclimatized in the laboratory for one month (*i.e.* kept in running aerated seawater, and feed with weeverfish flesh every two days). For the experiment, fish were individually separated in a flow-through seawater open system (40L fish^{-1}, daily renewed; 21.0 ± 0.5°C, mean ± SE, $n = 21$) under 12h:12h light:dark period. PVC pipes were used as shelter and experimental units were partially covered with opaque sheeting to respect the

lucifugal and benthic behaviour of eels (Baillon et al., 2016). The experimental procedures of the present study respect the animal ethical guidelines in order to secure a decent existence in laboratory and reduce suffering according to the French Ministry of Higher Education and Research.

Synthesis and characterization of PEG-coated gold nanoparticles - Polyethylene glycol coated gold nanoparticles (AuNP) were prepared according to Brisson and Mornet method (Brisson and Mornet, 2009). Briefly, gold ions were reduced in sodium citrate solution in order to synthesize 10nm-sized and citrate-coated gold nanoparticles. Based on the surface ligand exchanges, polyethylene glycol (PEG) were then substituted to citrate. The PEG-coated AuNPs solution reached a gold concentration of 2.15 g Au L^{-1} corresponding to 2.1×10^{17} nanoparticles L^{-1}. TEM micrograph of the AuNP prior to their incorporation into fish food was observed (figure 1). The synthesized AuNP looked uniform with a narrow size distribution (10 ± 1 nm) (see (Perrier et al., 2018)). The AuNP were stabilized with PEG-amine at the particle surface and zeta potential was about 40 mV at pH 7, corresponding to a positive charge.

Spiked food preparation - Artificial food spiked with PEG-coated AuNPs was prepared from weeverfish (*Trachinus sp.*) caught in the Arcachon Bay. Weeverfish flesh was crushed and mixed with dissolved agar-agar (0.8% of total food weight, Sigma-Aldrich, Missouri, U.S) to obtain a homogeneous mixture before the addition of AuNPs solution. For control diet, AuNPs solution was replaced by an equal volume of ultra-pure water. Nominal concentrations in gold spiked food were defined as NP0 for control, NP1 for 1 mg Au.kg^{-1} fresh weight (fw), and NP10 for 10 mg Au.kg^{-1} fw. So as to get standardized food portions, final preparation was divided to fill identical molds and stored at -20°C until use. One food portion corresponded to 11 ± 3 g fw (mean $\pm$ SE, n = 15). Gold

concentrations in the diet were confirmed as described further and were lower than the detection limit for NP0, 0.98 ± 0.03 for NP1 and 11.96 ± 0.84 mg Au.kg^{-1} fw for NP10 (mean $\pm$ SE, $n = 5$).

Experimental design - Each eel was fed with one standardized portion every two days at dusk for 21 days (*i.e.* 11 meals). The unconsumed food was removed the next morning, dried at 45°C for 48 hours and weighed to assess fish feeding behaviour and food consumption. Water monitoring did not reveal the presence of gold in water tanks enabling to consider exposure of fish only by the trophic route. After 21 days of exposure, six eels from each condition were sacrificed and tissues (blood, brain, gills, heart, intestine, kidney, liver, muscle, spleen) were dissected. Morphometric parameters were measured for each eel to calculate the following fish indices: Fulton condition factor as [(total weigh (g) ÷ total length^3 (cm)) × 100] and Hepato-Somatic Index (HSI), Spleen somatic Index (SSI), and Intestine Somatic index (ISI) as [(mass of the organ (g) ÷ total weigh (g)) × 100]. Intestine tissues were manually emptied during dissection to remove most of the food bowl and reduce interindividual variability. All organs were stored at -20°C until gold quantification analysis. A standardized sample of liver and the whole brain were stored in RNA-later solution for further RNA-sequencing analyses.

Gold quantification – The method was adapted from previous work (Perrier et al., 2018) as follows. Biological samples were dried (48 h at 45°C) and then digested in *aqua regia* (0.25 volume of 65% HNO$_3$ - Carlo Erba Reagent, Dasit Group, Italy - and 0.75 volume of 37% HCl - SCP Science, Canada) at 100°C for 3 h. Muscle and food samples (weighing > 100 mg dry weight) were digested in 5 mL of *aqua regia*; blood, liver and kidney (tissues weight between 50 and 100 mg dw) in 3 mL of *aqua regia*; intestine (tissues weight between 10 and 30 mg dw) in 2 mL of *aqua regia*; brain, heart, gills and

spleen (weighing < 10 mg dw) in 1 mL of *aqua regia.* All acid-digested samples were diluted 6:1 with ultrapure water (MilliQ, Bedford, MA, USA). Gold concentrations were expressed as µg Au g^{-1} dw. The water samples were diluted with ultrapure acidified water (2% *aqua regia*) prior gold quantifications. Gold quantifications in fish tissues were performed by HR-ICP-MS (Element XR, Thermo Scientific) at the GET laboratory in Toulouse, France. The detection limit of the Element XR in fish digests was around 0.1 ng L^{-1} for gold. Water gold concentrations in experimental tanks were determined by electrothermic atomic absorption spectrophotometry with Zeeman correction using a graphite furnace (240Z AA spectrometer, Agilent Technologies, USA), of which detection limit was 0.1 µg Au L^{-1}. The analytical method was validated by the analyses of gold standard solutions (Merck, Darmstadt, Germany), and for each samples series by checking an inter-laboratories biological reference material (gold contaminated asiatic clam *Corbicula fluminea*, concentration intercalibrated with six laboratories, data not shown). Gold recoveries reached 101 ± 1 % ($n = 26$).

After the 21-day exposure, the following formula was used to assess trophic transfer ratio: [(organ gold quantity in fish ÷ ingested gold quantity) × 100].

RNA-sequencing analyses and bioinformatics pipeline - Total RNAs were extracted from liver and brain of NP0 (n=6) and NP1 (n=6) animals (eels fed at NP0 and at NP1 respectively) using SV Total RNA Isolation System (Promega) according to the manufacturer's instructions, leading to a total of 24 RNA samples. NP10 eels were excluded for RNA-sequencing analyses. The 24 RNA-sequencing libraries were prepared by Genotoul (France) in order to perform analyses with the Illumina HiSeq 3000 technology. Raw RNA sequencing reads were deposited in NCBI Gene Expression Omnibus under GEO accession GSE110011.

The read quality of the RNA-seq libraries was evaluated using FastQC (Andrews, 2010). Cleaned and filtered reads were *de novo* assembled using the Trinity assembler version 2.0.6 and the DRAP procedure version 1.7 (Cabau et al., 2017). The resulting contigs were aligned with NCBI blastx program (version 2.2.26) with an E-value of 1e-5 against Refseq protein, Swissprot and Ensembl protein reference files from *Danio rerio*, *Latimeria chalumnae* and *Lepisosteus oculatus* to retrieve the best annotation. Ribosomal genes, repeat sequences, gene ontology and structural annotation were assessed as in previous work (Bertucci et al., 2017). RNA-sequencing results were validated by RT-qPCR. Specific primers amplifying 90-110 bp were designed for a set of 8 genes using the software primer3 (Untergasser et al., 2012) (details are given in electronic supplementary information ESI.1). These targets were chosen randomly and spanned a range of fold change values similar to the entire set of transcripts (see supplementary information ESI.3 and ESI.4). Amplicons lengths were checked by agarose gel electrophoresis after PCR amplification using the GoTaq DNA Polymerase (Promega) following manufacturer's protocol. Primer efficiencies were determined using standard curve analysis ($E = 10^{(-1/\text{slope})}$) with a dilution series of pooled cDNA from all conditions and ranged from 84% to 106%. Transcript level quantification was performed using the GoTaq qPCR mastermix from Promega and a Startagene Mx3000P system. PCR conditions were as follows: 1X GoTaq qPCR mastermix (Promega), 200 nM primers and 10 ng of cDNA in a total volume of 25 μL. PCR parameters were: 95 °C for 2 min, followed by 40–45 cycles of 15 s at 95 °C, 60 s at 60 °C and a dissociation curve step (60–95 °C) to confirm the amplification of a unique products and the absence of primer dimers. The gene encoding for the elongation factor 1-alpha was selected as control gene based on its stability in the RNA-seq data set. The relative quantification for each gene

was normalized by its expression level and relative to the NP0 condition. Fold expression values were calculated as $(E^{dCT})_{target}/(E^{dCT})_{control}$ where E is the amplification efficiency for each pair of primers and $dCT = CT_{NP0} - CT_{NP1}$. Agreement between RNAseq results and qPCR was strong, with a R^2 value of 0.9 (electronic supplementary information ESI.1).

Statistical analysis - Data were processed using R 3.3.0 collaborative statistical software (www.r-project.org/). After checking for normality and homoscedasticity of error terms, comparisons among groups were performed using analysis of variance (ANOVA, $p<0.05$) and pairwise differences were identified by a SNK test. Otherwise, a Kruskall-Wallis procedure followed by t-tests was applied. Differential gene expressions between NP0 and NP1 eels were based on reads counts by using DESeq2 R package (Love et al., 2014). Data quality assessment and quality control of the count matrix were performed by sample clustering and are presented in electronic supplementary information ESI.2. P-values for differential gene expressions were corrected for multiple testing using the Benjamini and Hochberg method and a false discovery rate (FDR) of 0.05 was used. Gene ontology (GO) annotations were obtained with an E-value and a homology threshold set to 10^{-6} and 50%, respectively. GO analyses were performed with Blas2GO 2.8 software (Gotz et al., 2008) and the topGO R package (Alexa and Rahnenfuhrer, 2019). In a matter of clarity, the redundancy in GO term was reduced with GO Trimming (Jantzen et al., 2011).

RESULTS

Mortality, morphometric indices and feeding behaviour - No mortality occurred during this experiment. Regarding the food consumption (table 1), no significant difference was observed between NP0 and NP1 eels that consumed between 86.75% and 100.00% of the

total amount of food provided during the experiment. However, half the NP10 eels nearly stopped feeding immediately from the beginning of the experiment, consuming only 6.75% to 19.74% of their food, while the other half fed normally (96.45% - 100%). That led to a significant difference in comparison to control and NP10 (*p value* = 0.04). We thus decided to exclude the NP10 group from the subsequent analysis in order to avoid misinterpretation of the results. At the end of experiment, we observed no significant differences in the total weight of NP0 and NP1 animals (table 1). However, although not significant, we noticed that NP1 eels gained almost twice less weight per gram of food consumed than NP0 eels. Amongst organosomatic indices, the intestine somatic index (ISI) and the spleen somatic index (SSI) were significantly lower after 21 days in NP1 samples compared to controls.

Gold accumulation in eel tissues - Gold concentrations were below the detection limits for all organs (brain, gills, heart, spleen, muscle and blood) except for intestine, kidney and liver (figure 2). No difference was observed in liver (NP0 = 0.010 ± 0.003 µg Au.mg^{-1}; NP1=0.015 ± 0.005 µg Au.mg^{-1}; p.value = 0.200). Statistical differences in gold accumulation were observed in intestine (NP0 = 0.008 ± 0.002 µg Au.mg^{-1}; NP1 = 0.090 ± 0.030 µg Au.mg^{-1}; p.value = 0.004) and kidney (NP0 = 0.012 ± 0.002 µg Au.mg^{-1}; NP1 = 0.039 ± 0.017 µg Au.mg^{-1}; p.value = 0.037) where Au concentration increased by approximately 11-times and 3-times compared to controls, respectively. Based on food consumptions of eels, we calculated that the transfer ratios of Au from food to each organ studied in NP1 condition were low with mean values of 0.0027% and 0.0031% for intestine and kidney, respectively.

Overview of transcriptomic responses - The 24 cDNA libraries were sequenced on a Hiseq3000 platform (Genotoul, Toulouse, France) and resulted in a total of 1.5 billion

paired reads of 150bp on average that were *de novo* assembled in a transcriptome made of 50,640 contigs (sequences) with a N50 of 3,231 bp. A total of 30,055 contigs (59.35 %) exhibited high homologies with known sequences (blastx evalue $1.E^{-5}$) amongst which 17,806 (59.24 %) were assigned to a gene ontology term. This Transcriptome Shotgun Assembly project has been deposited at DDBJ/EMBL/GenBank under the accession GGGR00000000. In spite of the lack of bioaccumulation of AuNP, trophic exposure led to significant differences in the transcription profile of a small proportion of the whole transcriptome (less than 1%) as 156 and 258 sequences were differentially expressed in brain and liver, respectively, compared to control eels (figure 3). The number of differentially transcribed genes (DEGs) was higher in the liver than in the brain. In the liver, genes were mostly down regulated, while in the brain, distributions between under- and over-expressed appeared more homogeneous. The complete list of DEGs is provided as electronic supplementary information (ESI.3 for the liver tissue and ESI.4 for the brain tissue).

Affected biological process - DEGs were annotated with GO terms (figure 4). In the significantly most represented GO terms (p value ≤ 0.05) amongst liver DEGs, we found terms related to immune system (*e.g.* GO:0006955, GO:0019882) and signal transduction (*e.g.* GO:0007165 and GO:0035556) with 12 and 21 differentially expressed sequences, respectively (Table 2). Similar GO terms were enriched in the brain DEG but to a lesser extent (figure 4), suggesting a common response to AuNP exposure in both organs (GO:0002474 and GO:0001916 for immunity-related terms, and GO:0032006 for signal transduction).

Common transcriptomic responses between liver and brain tissues - DEGs between NP0 and NP1 eels were compared for the liver and brain in order to highlight a specific and

common transcriptomic response to AuNP trophic exposure. Seventeen regulated genes, encoding 13 putative proteins, were shared between the two tissues (table 3). In particular, Scya112, Mr1, Nlrc3 and Nlrp12 proteins were involved in immune responses, and Lamtor3, Napb and Sptbn1 proteins were involved in cellular movements. Interestingly, genes encoding two proteins involved in the inflammasome (*nlrc3* and *nlrp12*) were jointly over-expressed in both liver and brain of NP1 eels. Overall, gene expression profiles were similar for both organs except for *tnrc6b* gene that is involved in RNA-mediated gene silencing.

DISCUSSION

The current production volumes of engineered nanomaterials are extremely uncertain with large discrepancies between surveys and literature. In absence of straightforward analytical methods, environmental concentrations of some NP materials could be predicted thanks to computational modelling based on levels of production. These models showed that in the most exposed European rivers, current levels of AgNP; ZnNP and TiNP might exceed 2 ng.L^{-1}; 300 ng.L^{-1} and 4 µg.L^{-1}, respectively (Bundschuh et al., 2018; Dumont et al., 2015; McGillicuddy et al., 2017). Due to a lower usage, concentrations of AuNP are expected to be even lower. In the same manner, not much work is reported on their environmental persistence/degradation, mostly due to the fact that quantification and characterization methods in environmental samples are still developing (Zänker and Schierz, 2012). The experiment presented here aimed to study the potential transfer of food-borne gold nanoparticles (AuNPs) to organs in European eels and the subsequent transcriptomic response by means of a RNA-sequencing approach. The exposure doses of 1 and 10 mg AuNP per kg of food (fresh weight) were chosen based on previous work in which significant transfer was observed from

contaminated algal suspension or biofilm to invertebrates and grazer fish that can

constitute prey for eels in the wild (Baudrimont et al., 2018; Perrier et al., 2018; Renault

et al., 2008). For instance, Asian clams *Corbicula fluminea* accumulated 4.3 µg Au.mg^{-1}

fw in their visceral mass when fed for 7 days with phytoplanktonic algae *Scenedesmus*

subspicatus contaminated with 4.65 mg.L^{-1} of AuNP, which is ten times lower than the

LC$_{50}$-24h for this algae. This may represents a bioconcentration factor of up to 26,000

(Renault et al., 2008). Then, the concentration of AuNP tested here could well result from

an environmental level in the ng.L^{-1} range. This is probably higher than the current level

but doesn't sound unrealistic should the production, use and release to nature of

engineered NP increase as predicted by 2050, with aquatic concentrations up to six times

higher than today (Giese et al., 2018).

These previous results suggested that the dietary route could be a major route of exposure

in a predator fish like *A. Anguilla*. We ensure that the food was the only source of NP

during the experiment and that no particles were naturally present in the water nor

released from spiked food (below detection limit).

Regarding the endpoints, no mortality was observed throughout this experiment. This

observation was consistent with a study involving dietary exposure of zebrafish (*Danio*

rerio) to gold nanoparticles (12 and 50 nm) (Geffroy et al., 2012). However, eels exposed

to high level of AuNPs (NP10) showed an erratic feeding behaviour which was not

observed in the NP0 and NP1 eels. A similar avoidance behaviour was pointed out in the

isopod *Porcellionides pruinosus* exposed to high levels of Ag nanoparticles (127 mg

Ag.kg^{-1}) by the trophic route (Tourinho et al., 2015). This discontinuation of feeding was

previously highlighted in fish facing high concentration of, or chronic exposure to metal

and organic contaminants (Kasumyan, 2001) and is considered as a nonspecific response

to NP stress. Gold quantification in eel tissues neither revealed significant bioaccumulation except for the intestine and kidney. Ramsden *et al.* (2009) showed an internal titanium transfer to rainbow trout after 10 weeks of TiO_2 nanoparticle-spiked food (10 and 100 mg.kg^{-1}), which get started from the fourth week according to the accumulation kinetics. Contrary to these results, gold transfer here was limited to intestine and kidney. This might be explained by the fact that we used (*i*) 10-fold lower exposure doses, (*ii*) a 3-fold shorter exposure period, (*iii*) a 3-fold bigger fish and (*iv*) different chemical nanoparticles. Despite the removal of intestinal contents prior to gold analysis, some food residuals might persist, restricting the ability to discern AuNP ad- or absorption to/on the digestive tract. However, this result clearly emphasized an exposure of eel intestinal barrier to AuNP (NP1 condition). Even though excluded from our analysis, this effect on intestinal barrier might partly explain the impairment in feeding behaviour of NP10 eels. In that case, one mode of action of AuNPs could be similar to the one that was observed in *Gammarus fossarum*, where AuNPs accumulated around and in intestinal cilia (Baudrimont et al., 2018) but this observation should be confirmed by future studies in predator fish. Moreover, impacts of NPs on eels were evidenced by lower ISI and SSI values of NP1 fish in comparison to controls. The reduction of the ISI, can be seen as a proxy of diet quality and the ability of organisms to absorb nutrients (Sanden et al., 2005). Changes in ISI due to poor quality and/or toxic food could result in enteritis-like condition characterized by changes in enterocyte structure and organization of mucosal folds, as well as the presence of numerous inflammatory cells in the digestive epithelium (Nordrum et al., 2000). Spleen was already found to be affected by AuNP (*i.e.* inflammatory lesions) in the grazer fish *Hypostomus plecostomus* fed with AuNP-contaminated biofilm (Perrier et al., 2018). We were not able to test whether the effects

observed here were due to gold as an ion or as a particle. According to literature, strong acidic conditions and high temperature are needed to favour the oxidation of Au(0) into Au(III) that forms toxic gold salts (Praharaj et al., 2007). Such conditions are unlikely met in the fish organs. Moreover, previous work demonstrated that AuNP located in lysosomal vesicles were not readily oxidized and that the low pH was just enough to pick up nanoparticle's coatings (Renault et al., 2008).

In term of transcriptomic changes in liver and brain, AuNP had impacts at the end of the 21-day exposure period for the NP1 compared to control eels despite low or not quantifiable rates of trophic transfer. For liver and brain, 258 (0.51% of the transcriptome) and 156 (0.31%) of the total genes were differentially expressed in NP1 eels compared to NP0 eels, respectively ($p<0.05$). If these transcriptomic alterations in the brain were confirmed and/or reinforced at higher concentration, we can hypothesize that they could result in behavioral changes responsible for the feeding reduction observed in NP10 eels. In the liver, the number of DEG is comparable with what was found in the liver of *D. rerio* exposed to water-borne Cd nanoparticles (Gao et al., 2018) or in *Sparus aurata* exposed to water-borne AuNP (Teles et al., 2019). Similarly, gene expression in zebrafish was altered even though no gold accumulation was detected in fish tissues after a 60-day trophic exposure experiment using AuNP-enriched food (Geffroy et al., 2012). For comparison, Cho *et al.* (2009a) investigated the gene expression response in mice liver after an intravenous administration of 4 or 100 nm PEG-coated AuNP (4.26 mg Au.kg^{-1} of body weight) for 30 minutes. Only 0.38% (for 4 nm) and 0.50% (for 100 nm) of the total genes were differentially expressed in AuNP exposed mice, highlighting relatively similar values to the present experiment, with similar chemical compositions of nanoparticles. In addition, authors pointed out that these genes were involved in

apoptosis, inflammation and metabolic processes (Cho et al., 2009b), showing again similarities in transcriptomic response despite differences among biological models and exposure conditions. The transcriptome-wide approach offered by RNA sequencing has proven its efficiency in ecotoxicology by exploring virtually all aspects of the physiology of an organism at once and in a single sample. However, since transcripts are not final products and effectors of gene expression, it's important, like what was done here, to couple transcriptomics with at least one appropriate endpoint at higher levels of biological organization in order to properly assess the potential occurrence of toxic events (Connon et al., 2012). Common endpoints include reproductive success, sex ratio, growth, survival, *etc*.

In the present study, the downregulation of several genes involved in the immune response were highlighted in the liver by gene ontology enrichment analysis which suggests an alteration of the immune status of NP1 eels. These results are in agreement with the lower SSI of NPs-exposed fish. In teleosts, the spleen is indeed the major source of antibodies production and immunological memory and fish with smaller SSI show lower immune response and disease resistance (Hadidi et al., 2008). Engineered nanoparticles were already reported to trigger an immune response (Dobrovolskaia and McNeil, 2007; Dwivedi et al., 2009; Ngobili and Daniele, 2016) and might interact with the immune system (García et al., 2013). In previous molecular studies, and similarly to the present results, this negative impact on the immune response of organisms was accompanied with the differential expression of genes involved in signal transduction, cytokine production and DNA repair regardless of NP structure or mode of exposure (Gao et al., 2018; Teles et al., 2019). These processes might highlight a common mode of action of metal NP. Whereas most of the previously cited examples only considered one

target organ (liver), we presently observed a common transcriptomic response in the brain. In particular, some DEGs encoded proteins of the NLR-receptor family (NLRC3 and NLRP12), a family of cytoplasmic proteins involved in many different biological processes including both innate and adaptive immunity (Kufer and Sansonetti, 2011). Mangan and Latz (2014) suggested that NLRC3 behaves as a watchdog to prevent an overshooting onset of immune responses in the wake of diverse immune stimuli. Both overexpressed in the liver and brain eel tissues, NLRP12 appeared as a critical checkpoint during inflammation, migration of immune cells and tumorigenesis (Allen et al., 2012). For example, a recent study pointed out the implication of NLRP12 in the inflammasome (Zaki et al., 2014), a multiprotein intracellular complex activated upon cellular infection or stress that triggers the highly pro-inflammatory cytokines. Several particulate materials, such as silica, asbestos, and carbon nanotubes, were also highlighted as inflammasome activators (Baron et al., 2015; Dostert et al., 2008; Naji et al., 2016). In addition, NLR subfamily might regulate the transcription of Major Histocompatibility Complex (MHC) proteins (Kobayashi and van den Elsen, 2012), a group of proteins located on cell surfaces and that are crucial for an effective adaptive immune response. Interestingly, MHC-related genes were found in the list of DEGs (table 2) and MHC appeared as an enriched cellular component in the liver of exposed eels (data not shown). In addition, a gene (*mr1*) encoding for an antigen-presenting molecule was also found to be down-regulated in both liver and brain tissues of exposed eels (table 3).

Considering that the gastrointestinal tract (i) was the first and the only biological barrier in direct contact with AuNPs, (ii) significantly accumulated Au and (iii) was significantly affected by NPs, as evidenced by lower ISI values of NPs-exposed fish, our results suggest that gut could be a start-point of the transcriptomic responses of exposed eels in

absence of quantifiable transfer to internal organs. Several other studies might support this hypothesis. First, nanoparticles might disrupt gut microbiota (Pietroiusti et al., 2016). For example, rats exhibited a shift in gut microbiome composition associated with changes in the expression of immunomodulatory genes after silver nanoparticles subchronic dietary exposure (Williams et al., 2015). Moreover, the activity of gut microbial populations also plays an important role in host health (Bennett et al., 2015) and the gut–liver axis emerges as an area of interest in the microbial-metabolic axis (Russell et al., 2013). Regarding the brain tissues, microbiota-gut-brain axis is also considered as a bidirectional communication which includes immune, endocrine and metabolic pathways (Dinan and Cryan, 2017). Moreover, present results highlighted a differential expression in both studied tissues of the *per3* gene, which encodes for a protein involved in biological rhythms. Thaiss *et al.* (2016) pointed out the bidirectional regulation between gut microbiota and rhythms, showing that disruption of homeostatic microbiome rhythmicity trigger genome-wide *de novo* oscillations in both intestine and liver tissues. Second, regarding dietary exposure, Bettini *et al.* (2017) reported a propensity of TiO_2 nanoparticles to generate immune responses in rat intestine by affecting dendritic cell frequencies and T-cell populations in the Peyer's patches. Here, RNA-sequencing results exhibited a clear immune response in the liver and brain tissues. Gastrointestinal tract is referred as playing an important role in immune function (Bergin and Witzmann, 2013) and might initiate immune response in the whole organism. For example, El Aidy *et al.* (2014) emphasized the implication of intestinal cytokines as a communication route in immune signalling from gut to brain. Finally, due to the presence of AuNPs in the digestive tract of exposed eels, disruption of digestive function might also be suspected, as previously reported by Guo *et al.* (2017) for TiO_2 nanoparticles.

Here, GO terms distribution in the liver (figure 4) exhibited numerous sequences associated with metabolic and biosynthetic processes. According to the literature, these results might suggest an impairment of digestive functions as a consequence of intestinal disorders engendered by AuNP exposure. In this view, although not significant, we must note that NP1 eels gained almost twice less weight per gram of food consumed than NP0 eels. However, a better understanding of the linkage between exposure to xenobiotics and adverse physiological outcomes is needed and certainly lies in future multidisciplinary studies that could include measurement of specific markers at the molecular, cellular and tissular levels. Based on the discussion above, we could suggest the measurement of cytokines production, profiling of gut microbiome and/or microscopy observation for instance. Such an approach is in agreement with conceptual frameworks like Adverse Outcome Pathways (Ankley et al., 2010) and systems biology (Kitano, 2002).

CONCLUSIONS

The present study aimed at understanding the transcriptomic response of liver and brain tissues of European eels exposed to diet-borne gold nanoparticles. Gold was poorly transferred from nanoparticles-enriched food to eels' organs. At the highest exposure level, eels presented an erratic feeding behaviour. Significant gold bioaccumulation was only detectable in the intestine and kidney of NP1 eels. Despite the absence of significant gold transfer to liver and brain, transcriptomic responses after AuNP trophic exposure were still revealed in these tissues (NP1), with some common genes differentially expressed in both organs. The genes affected by diet-borne exposure to AuNP were mainly involved in the immune system. These results are consistent with the current literature on NPs in fish. However, our study used lower NP doses, probably closer to what is likely present in natural aquatic environments. As proposed, the intestine tissue

might contribute to the transcriptomic responses observed in the liver and brain, emphasizing the necessity to study this tissue in future experiments.

Supplemental Data—The Supplemental Data are available on the Wiley Online Library at DOI: 10.1002/etc.xxxx.

Disclaimer— The authors declare that they have no known competing financial interests or personal relationships that could have appeared to influence the work reported in this paper.

Data availability statement—Data, associated metadata, and calculation tools are available from the corresponding author (magalie.baudrimont@u-bordeaux.fr). Raw RNA sequencing reads has been deposited in NCBI Gene Expression Omnibus under GEO accession GSE110011 and the Transcriptome Shotgun Assembly project has been deposited at DDBJ/EMBL/GenBank under the accession GGGR00000000.

REFERENCES

Abdelhalim, M.A.K., and Mady, M. (2012). Physical Properties of Different Gold Nanoparticles: Ultraviolet-Visible and Fluorescence Measurements. J. Nanomedicine Nanotechnol. *03*.

Alexa, A., and Rahnenfuhrer, J. (2019). topGO: Enrichment Analysis for Gene Ontology. R package version 2.36.0.

Allen, I.C., Wilson, J.E., Schneider, M., Lich, J.D., Roberts, R.A., Arthur, J.C., Woodford, R.-M.T., Davis, B.K., Uronis, J.M., Herfarth, H.H., et al. (2012). NLRP12 Suppresses Colon Inflammation and Tumorigenesis through the Negative Regulation of Noncanonical NF-κB Signaling. Immunity *36*, 742–754.

Andrews, S. (2010). FastQC: a quality control tool for high throughput sequence data. Available online at: http://www.bioinformatics.babraham.ac.uk/projects/fastqc.

Ankley, G.T., Bennett, R.S., Erickson, R.J., Hoff, D.J., Hornung, M.W., Johnson, R.D., Mount, D.R., Nichols, J.W., Russom, C.L., Schmieder, P.K., et al. (2010). Adverse outcome pathways: A conceptual framework to support ecotoxicology research and risk assessment. Environ. Toxicol. Chem. *29*, 730–741.

Baalousha, M., Yang, Y., Vance, M.E., Colman, B.P., McNeal, S., Xu, J., Blaszczak, J., Steele, M., Bernhardt, E., and Hochella, M.F. (2016). Outdoor urban nanomaterials: The emergence of a new, integrated, and critical field of study. Sci. Total Environ. *557–558*, 740–753.

Baillon, L., Pierron, F., Pannetier, P., Normandeau, E., Couture, P., Labadie, P., Budzinski, H., Lambert, P., Bernatchez, L., and Baudrimont, M. (2016). Gene transcription profiling in wild and laboratory-exposed eels: Effect of captivity and in situ chronic exposure to pollution. Sci. Total Environ. *571*, 92–102.

Baron, L., Gombault, A., Fanny, M., Villeret, B., Savigny, F., Guillou, N., Panek, C., Le Bert, M., Lagente, V., Rassendren, F., et al. (2015). The NLRP3 inflammasome is activated by nanoparticles through ATP, ADP and adenosine. Cell Death Dis. *6*, e1629–e1629.

Baudrimont, M., Andrei, J., Mornet, S., Gonzalez, P., Mesmer-Dudons, N., Gourves, P.-Y., Jaffal, A., Dedourge-Geffard, O., Geffard, A., Geffard, O., et al. (2018). Trophic transfer and effects of gold nanoparticles (AuNPs) in Gammarus fossarum from contaminated periphytic biofilm. Environ. Sci. Pollut. Res. *25*, 11181–11191.

Belpaire, C., Goemans, G., Geeraerts, C., Quataert, P., and Parmentier, K. (2008). Pollution fingerprints in eels as models for the chemical status of rivers. ICES J. Mar. Sci. *65*, 1483–1491.

Bennett, B.J., Hall, K.D., Hu, F.B., McCartney, A.L., and Roberto, C. (2015). Nutrition and the science of disease prevention: a systems approach to support metabolic health: Nutrition and the science of disease prevention. Ann. N. Y. Acad. Sci. *1352*, 1–12.

Bergin, I.L., and Witzmann, F.A. (2013). Nanoparticle toxicity by the gastrointestinal route: evidence and knowledge gaps. Int. J. Biomed. Nanosci. Nanotechnol. *3*.

Bertucci, A., Pierron, F., Thebault, J., Klopp, C., Bellec, J., Gonzalez, P., and Baudrimont, M. (2017). Transcriptomic responses of the endangered freshwater mussel Margaritifera margaritifera to trace metal contamination in the Dronne River, France. Env. Sci Pollut Res Int *24*, 27145–27159.

Bettini, S., Boutet-Robinet, E., Cartier, C., Coméra, C., Gaultier, E., Dupuy, J., Naud, N., Taché, S., Grysan, P., Reguer, S., et al. (2017). Food-grade TiO2 impairs intestinal and systemic immune homeostasis, initiates preneoplastic lesions and promotes aberrant crypt development in the rat colon. Sci. Rep. *7*, 40373.

de Boer, Jacob., van der Valk, Frank., Kerkhoff, M.A.T., Hagel, Paul., and Brinkman, U.A.Th. (1994). An 8-Year Study on the Elimination of PCBs and Other Organochlorine Compounds from Eel (Anguilla anguilla) under Natural Conditions. Environ. Sci. Technol. *28*, 2242–2248.

Brisson, A., and Mornet, S. (2009). Functionalization of gold nanoparticles with oriented proteins. Application to the high-density labelling of cell membranes (European patent EP2018559A1).

Bundschuh, M., Filser, J., Lüderwald, S., McKee, M.S., Metreveli, G., Schaumann, G.E., Schulz, R., and Wagner, S. (2018). Nanoparticles in the environment: where do we come from, where do we go to? Environ. Sci. Eur. *30*, 6.

Caballero-Guzman, A., and Nowack, B. (2016). A critical review of engineered nanomaterial release data: Are current data useful for material flow modeling? Environ. Pollut. Barking Essex 1987 *213*, 502–517.

Cabau, C., Escudié, F., Djari, A., Guiguen, Y., Bobe, J., and Klopp, C. (2017). Compacting and correcting Trinity and Oases RNA-Seq *de novo* assemblies. PeerJ *5*, e2988.

Cardoso, E., Rezin, G.T., Zanoni, E.T., de Souza Notoya, F., Leffa, D.D., Damiani, A.P., Daumann, F., Rodriguez, J.C.O., Benavides, R., da Silva, L., et al. (2014). Acute and chronic administration of gold nanoparticles cause DNA damage in the cerebral cortex of adult rats. Mutat. Res. Mol. Mech. Mutagen. *766–767*, 25–30.

Cedervall, T., Hansson, L.-A., Lard, M., Frohm, B., and Linse, S. (2012). Food Chain Transport of Nanoparticles Affects Behaviour and Fat Metabolism in Fish. PLoS ONE *7*, e32254.

Cheng, Y., Dai, Q., Morshed, R.A., Fan, X., Wegscheid, M.L., Wainwright, D.A., Han, Y., Zhang, L., Auffinger, B., Tobias, A.L., et al. (2014). Blood-Brain Barrier Permeable Gold Nanoparticles: An Efficient Delivery Platform for Enhanced Malignant Glioma Therapy and Imaging. Small n/a-n/a.

Chichova, M., Shkodrova, M., Vasileva, P., Kirilova, K., and Doncheva-Stoimenova, D. (2014). Influence of silver nanoparticles on the activity of rat liver mitochondrial ATPase. J. Nanoparticle Res. *16*, 2243.

Cho, W.-S., Kim, S., Han, B.S., Son, W.C., and Jeong, J. (2009a). Comparison of gene expression profiles in mice liver following intravenous injection of 4 and 100nm-sized PEG-coated gold nanoparticles. Toxicol. Lett. *191*, 96–102.

Cho, W.-S., Kim, S., Han, B.S., Son, W.C., and Jeong, J. (2009b). Comparison of gene expression profiles in mice liver following intravenous injection of 4 and 100nm-sized PEG-coated gold nanoparticles. Toxicol. Lett. *191*, 96–102.

Connon, R.E., Geist, J., and Werner, I. (2012). Effect-Based Tools for Monitoring and Predicting the Ecotoxicological Effects of Chemicals in the Aquatic Environment. Sensors *12*, 12741–12771.

Costa, L., Mohmood, I., Trindade, T., Anjum, N.A., Duarte, A.C., and Pereira, E. (2016). Phagocytic cell responses to silica-coated dithiocarbamate-functionalized iron oxide nanoparticles and mercury co-exposures in Anguilla anguilla L. Environ. Sci. Pollut. Res. *23*, 12272–12286.

Costa, L.C., Mohmood, I., Trindade, T., Saleem, M., Duarte, A.C., Pereira, E., and Ahmad, I. (2015). Rescheduling the process of nanoparticle removal used for water mercury remediation can increase the risk to aquatic organism: evidence of innate immune functions modulation in European eel (Anguilla anguilla L.). Environ. Sci. Pollut. Res. Int. *22*, 18574–18589.

Croteau, M.-N., Dybowska, A.D., Luoma, S.N., and Valsami-Jones, E. (2011). A novel approach reveals that zinc oxide nanoparticles are bioavailable and toxic after dietary exposures. Nanotoxicology *5*, 79–90.

Dinan, T.G., and Cryan, J.F. (2017). Gut instincts: microbiota as a key regulator of brain development, ageing and neurodegeneration: Microbiota-gut-brain axis across the lifespan. J. Physiol. *595*, 489–503.

Dobrovolskaia, M.A., and McNeil, S.E. (2007). Immunological properties of engineered nanomaterials. Nat. Nanotechnol. *2*, 469–478.

Dostert, C., Petrilli, V., Van Bruggen, R., Steele, C., Mossman, B.T., and Tschopp, J. (2008). Innate Immune Activation Through Nalp3 Inflammasome Sensing of Asbestos and Silica. Science *320*, 674–677.

Dumont, E., Johnson, A.C., Keller, V.D.J., and Williams, R.J. (2015). Nano silver and nano zinc-oxide in surface waters – Exposure estimation for Europe at high spatial and temporal resolution. Environ. Pollut. *196*, 341–349.

Dwivedi, P.D., Misra, A., Shanker, R., and Das, M. (2009). Are nanomaterials a threat to the immune system? Nanotoxicology *3*, 19–26.

El Aidy, S., Dinan, T.G., and Cryan, J.F. (2014). Immune modulation of the brain-gut-microbe axis. Front. Microbiol. *5*.

Ferreira, P., Fonte, E., Soares, M.E., Carvalho, F., and Guilhermino, L. (2016). Effects of multi-stressors on juveniles of the marine fish Pomatoschistus microps: Gold nanoparticles, microplastics and temperature. Aquat. Toxicol. Amst. Neth. *170*, 89–103.

Ferry, J.L., Craig, P., Hexel, C., Sisco, P., Frey, R., Pennington, P.L., Fulton, M.H., Scott, I.G., Decho, A.W., Kashiwada, S., et al. (2009). Transfer of gold nanoparticles from the water column to the estuarine food web. Nat. Nanotechnol. *4*, 441–444.

Fouqueray, M., Dufils, B., Vollat, B., Chaurand, P., Botta, C., Abacci, K., Labille, J., Rose, J., and Garric, J. (2012). Effects of aged TiO2 nanomaterial from sunscreen on Daphnia magna exposed by dietary route. Environ. Pollut. *163*, 55–61.

Freese, C., Uboldi, C., Gibson, M.I., Unger, R.E., Weksler, B.B., Romero, I.A., Couraud, P.-O., and Kirkpatrick, C. (2012). Uptake and cytotoxicity of citrate-coated gold nanospheres: Comparative studies on human endothelial and epithelial cells. Part. Fibre Toxicol. *9*, 23.

Gao, M., Lv, M., Liu, Y., and Song, Z. (2018). Transcriptome analysis of the effects of Cd and nanomaterial-loaded Cd on the liver in zebrafish. Ecotoxicol. Environ. Saf. *164*, 530–539.

Garacci, M., Barret, M., Folgoas, C., Flahaut, E., Chimowa, G., Bertucci, A., Gonzalez, P., Silvestre, J., Gauthier, L., Zouine, M., et al. (2019). Transcriptomic response of the benthic freshwater diatom Nitzschia palea exposed to Few Layer Graphene. Environ. Sci. Nano *6*, 1363–1381.

García, C.P., Sumbayev, V., Gilliland, D., Yasinska, I.M., Gibbs, B.F., Mehn, D., Calzolai, L., and Rossi, F. (2013). Microscopic Analysis of the Interaction of Gold Nanoparticles with Cells of the Innate Immune System. Sci. Rep. *3*, 1326.

Geeraerts, C., and Belpaire, C. (2010). The effects of contaminants in European eel: a review. Ecotoxicology *19*, 239–266.

Geffroy, B., Ladhar, C., Cambier, S., Treguer-Delapierre, M., Brèthes, D., and Bourdineaud, J.-P. (2012). Impact of dietary gold nanoparticles in zebrafish at very low contamination pressure: The role of size, concentration and exposure time. Nanotoxicology *6*, 144–160.

Giese, B., Klaessig, F., Park, B., Kaegi, R., Steinfeldt, M., Wigger, H., von Gleich, A., and Gottschalk, F. (2018). Risks, Release and Concentrations of Engineered Nanomaterial in the Environment. Sci. Rep. *8*, 1565.

Gliga, A.R., Skoglund, S., Odnevall Wallinder, I., Fadeel, B., and Karlsson, H.L. (2014). Size-dependent cytotoxicity of silver nanoparticles in human lung cells: the role of cellular uptake, agglomeration and Ag release. Part. Fibre Toxicol. *11*, 11.

Gotz, S., Garcia-Gomez, J.M., Terol, J., Williams, T.D., Nagaraj, S.H., Nueda, M.J., Robles, M., Talon, M., Dopazo, J., and Conesa, A. (2008). High-throughput functional annotation and data mining with the Blast2GO suite. Nucleic Acids Res. *36*, 3420–3435.

Guo, Z., Martucci, N.J., Moreno-Olivas, F., Tako, E., and Mahler, G.J. (2017). Titanium dioxide nanoparticle ingestion alters nutrient absorption in an in vitro model of the small intestine. NanoImpact *5*, 70–82.

Hadidi, S., Glenney, G.W., Welch, T.J., Silverstein, J.T., and Wiens, G.D. (2008). Spleen size predicts resistance of rainbow trout to Flavobacterium psychrophilum challenge. J. Immunol. Baltim. Md 1950 *180*, 4156–4165.

Hofmann-Amtenbrink, M., Grainger, D.W., and Hofmann, H. (2015). Nanoparticles in medicine: Current challenges facing inorganic nanoparticle toxicity assessments and standardizations. Nanomedicine Nanotechnol. Biol. Med. *11*, 1689–1694.

Huerta-García, E., Pérez-Arizti, J.A., Márquez-Ramírez, S.G., Delgado-Buenrostro, N.L., Chirino, Y.I., Iglesias, G.G., and López-Marure, R. (2014). Titanium dioxide nanoparticles induce strong oxidative stress and mitochondrial damage in glial cells. Free Radic. Biol. Med. *73*, 84–94.

Jantzen, S.G., Sutherland, B.J., Minkley, D.R., and Koop, B.F. (2011). GO Trimming: Systematically reducing redundancy in large Gene Ontology datasets. BMC Res. Notes *4*, 267.

Jeevanandam, J., Barhoum, A., Chan, Y.S., Dufresne, A., and Danquah, M.K. (2018). Review on nanoparticles and nanostructured materials: history, sources, toxicity and regulations. Beilstein J. Nanotechnol. *9*, 1050–1074.

Kasumyan, A.O. (2001). Effects of chemical pollutants on foraging behavior and sensitivity of fish to food stimuli. J. Ichthyol. *41*, 76–87.

Kimling, J., Maier, M., Okenve, B., Kotaidis, V., Ballot, H., and Plech, A. (2006). Turkevich Method for Gold Nanoparticle Synthesis Revisited. J. Phys. Chem. B *110*, 15700–15707.

Kitano, H. (2002). Systems Biology: A Brief Overview. Science *295*, 1662–1664.

Kobayashi, K.S., and van den Elsen, P.J. (2012). NLRC5: a key regulator of MHC class I-dependent immune responses. Nat. Rev. Immunol. *12*, 813–820.

Kufer, T.A., and Sansonetti, P.J. (2011). NLR functions beyond pathogen recognition. Nat. Immunol. *12*, 121–128.

Ladhar, C., Geffroy, B., Cambier, S., Treguer-Delapierre, M., Durand, E., Brèthes, D., and Bourdineaud, J.-P. (2014). Impact of dietary cadmium sulphide nanoparticles on *Danio rerio* zebrafish at very low contamination pressure. Nanotoxicology *8*, 676–685.

Larguinho, M., Correia, D., Diniz, M.S., and Baptista, P.V. (2014). Evidence of one-way flow bioaccumulation of gold nanoparticles across two trophic levels. J. Nanoparticle Res. *16*, 2549.

Love, M.I., Huber, W., and Anders, S. (2014). Moderated estimation of fold change and dispersion for RNA-seq data with DESeq2. Genome Biol. *15*, 550.

Mangan, M.S.J., and Latz, E. (2014). NLRC3 Puts the Brakes on STING. Immunity *40*, 305–306.

McGillicuddy, E., Murray, I., Kavanagh, S., Morrison, L., Fogarty, A., Cormican, M., Dockery, P., Prendergast, M., Rowan, N., and Morris, D. (2017). Silver nanoparticles in the environment: Sources, detection and ecotoxicology. Sci. Total Environ. *575*, 231–246.

McTeer, J., Dean, A.P., White, K.N., and Pittman, J.K. (2014). Bioaccumulation of silver nanoparticles into *Daphnia magna* from a freshwater algal diet and the impact of phosphate availability. Nanotoxicology *8*, 305–316.

Naji, A., Muzembo, B.A., Yagyu, K., Baba, N., Deschaseaux, F., Sensebé, L., and Suganuma, N. (2016). Endocytosis of indium-tin-oxide nanoparticles by macrophages provokes pyroptosis requiring NLRP3-ASC-Caspase1 axis that can be prevented by mesenchymal stem cells. Sci. Rep. *6*, 26162.

Ngobili, T.A., and Daniele, M.A. (2016). Nanoparticles and direct immunosuppression. Exp. Biol. Med. *241*, 1064–1073.

Nordrum, S., Bakke-McKellep, A.M., Krogdahl, A., and Buddington, R.K. (2000). Effects of soybean meal and salinity on intestinal transport of nutrients in Atlantic salmon (Salmo salar L.) and rainbow trout (Oncorhynchus mykiss). Comp. Biochem. Physiol. B Biochem. Mol. Biol. *125*, 317–335.

Nowack, B., Brouwer, C., Geertsma, R.E., Heugens, E.H.W., Ross, B.L., Toufektsian, M.-C., Wijnhoven, S.W.P., and Aitken, R.J. (2012). Analysis of the occupational, consumer and environmental exposure to engineered nanomaterials used in 10 technology sectors. Nanotoxicology *7*, 1152–1156.

OECD (2010). List of Manufactured Nanomaterials and List of Endpoints for Phase One
of the Sponsorship Programme for the Testing of Manufactured Nanomaterials:
Revision. 16 p.

Park, E.-J., Kim, H., Kim, Y., Yi, J., Choi, K., and Park, K. (2010). Inflammatory
responses may be induced by a single intratracheal instillation of iron nanoparticles in
mice. Toxicology *275*, 65–71.

Perrier, F., Baudrimont, M., Mornet, S., Mesmer-Dudons, N., Lacomme, S., Etcheverria,
B., Simon, O., and Feurtet-Mazel, A. (2018). Gold nanoparticle trophic transfer from
natural biofilm to grazer fish. Gold Bull. *51*, 163–173.

Pierron, F., Baudrimont, M., Lucia, M., Durrieu, G., Massabuau, J.-C., and Elie, P.
(2008). Cadmium uptake by the European eel: Trophic transfer in field and
experimental investigations. Ecotoxicol. Environ. Saf. *70*, 10–19.

Pietroiusti, A., Magrini, A., and Campagnolo, L. (2016). New frontiers in
nanotoxicology: Gut microbiota/microbiome-mediated effects of engineered
nanomaterials. Toxicol. Appl. Pharmacol. *299*, 90–95.

Praharaj, S., Panigrahi, S., Basu, S., Pande, S., Jana, S., Ghosh, S.K., and Pal, T. (2007).
Effect of bromide and chloride ions for the dissolution of colloidal gold. J. Photochem.
Photobiol. Chem. *187*, 196–201.

Qiu, T.A., Bozich, J.S., Lohse, S.E., Vartanian, A.M., Jacob, L.M., Meyer, B.M.,
Gunsolus, I.L., Niemuth, N.J., Murphy, C.J., Haynes, C.L., et al. (2015). Gene
expression as an indicator of the molecular response and toxicity in the bacterium
Shewanella oneidensis and the water flea Daphnia magna exposed to functionalized
gold nanoparticles. Environ. Sci. Nano *2*, 615–629.

Ramsden, C.S., Smith, T.J., Shaw, B.J., and Handy, R.D. (2009). Dietary exposure to titanium dioxide nanoparticles in rainbow trout, (Oncorhynchus mykiss): no effect on growth, but subtle biochemical disturbances in the brain. Ecotoxicology *18*, 939–951.

Renault, S., Baudrimont, M., Mesmer-Dudons, N., Gonzalez, P., Mornet, S., and Brisson, A. (2008). Impacts of gold nanoparticle exposure on two freshwater species: a phytoplanktonic alga (Scenedesmus subspicatus) and a benthic bivalve (Corbicula fluminea). Gold Bull. *41*, 116–126.

Russell, W.R., Hoyles, L., Flint, H.J., and Dumas, M.-E. (2013). Colonic bacterial metabolites and human health. Curr. Opin. Microbiol. *16*, 246–254.

Sanden, M., Berntssen, M.H.G., Krogdahl, A., Hemre, G.-I., and Bakke-McKellep, A.-M. (2005). An examination of the intestinal tract of Atlantic salmon, Salmo salar L., parr fed different varieties of soy and maize. J. Fish Dis. *28*, 317–330.

Shrivastava, R., Raza, S., Yadav, A., Kushwaha, P., and Flora, S.J.S. (2014). Effects of sub-acute exposure to TiO_2, ZnO and Al_2O_3 nanoparticles on oxidative stress and histological changes in mouse liver and brain. Drug Chem. Toxicol. *37*, 336–347.

Srikanth, K., Anjum, N.A., Trindade, T., Duarte, A.C., Pereira, E., and Ahmad, I. (2015). Lipid peroxidation and its control in Anguilla anguilla hepatocytes under silica-coated iron oxide nanoparticles (with or without mercury) exposure. Environ. Sci. Pollut. Res. Int. *22*, 9617–9625.

Tangaa, S.R., Selck, H., Winther-Nielsen, M., and Khan, F.R. (2016). Trophic transfer of metal-based nanoparticles in aquatic environments: a review and recommendations for future research focus. Environ. Sci. Nano *3*, 966–981.

Teles, M., Fierro-Castro, C., Na-Phatthalung, P., Tvarijonaviciute, A., Trindade, T., Soares, A.M.V.M., Tort, L., and Oliveira, M. (2016). Assessment of gold nanoparticle

effects in a marine teleost (Sparus aurata) using molecular and biochemical biomarkers. Aquat. Toxicol. *177*, 125–135.

Teles, M., Soares, A.M.V.M., Tort, L., Guimarães, L., and Oliveira, M. (2017). Linking cortisol response with gene expression in fish exposed to gold nanoparticles. Sci. Total Environ. *584–585*, 1004–1011.

Teles, M., Reyes-López, F.E., Balasch, J.C., Tvarijonaviciute, A., Guimarães, L., Oliveira, M., and Tort, L. (2019). Toxicogenomics of Gold Nanoparticles in a Marine Fish: Linkage to Classical Biomarkers. Front. Mar. Sci. *6*.

Thaiss, C.A., Levy, M., Korem, T., Dohnalová, L., Shapiro, H., Jaitin, D.A., David, E., Winter, D.R., Gury-BenAri, M., Tatirovsky, E., et al. (2016). Microbiota Diurnal Rhythmicity Programs Host Transcriptome Oscillations. Cell *167*, 1495-1510.e12.

Tourinho, P.S., van Gestel, C.A.M., Jurkschat, K., Soares, A.M.V.M., and Loureiro, S. (2015). Effects of soil and dietary exposures to Ag nanoparticles and AgNO3 in the terrestrial isopod Porcellionides pruinosus. Environ. Pollut. *205*, 170–177.

Untergasser, A., Cutcutache, I., Koressaar, T., Ye, J., Faircloth, B.C., Remm, M., and Rozen, S.G. (2012). Primer3—new capabilities and interfaces. Nucleic Acids Res. *40*, e115–e115.

Volland, M., Hampel, M., Martos-Sitcha, J.A., Trombini, C., Martínez-Rodríguez, G., and Blasco, J. (2015). Citrate gold nanoparticle exposure in the marine bivalve Ruditapes philippinarum: uptake, elimination and oxidative stress response. Environ. Sci. Pollut. Res. Int. *22*, 17414–17424.

Wang, Z., Yin, L., Zhao, J., and Xing, B. (2016). Trophic transfer and accumulation of TiO2 nanoparticles from clamworm (Perinereis aibuhitensis) to juvenile turbot (Scophthalmus maximus) along a marine benthic food chain. Water Res. *95*, 250–259.

Williams, K., Milner, J., Boudreau, M.D., Gokulan, K., Cerniglia, C.E., and Khare, S. (2015). Effects of subchronic exposure of silver nanoparticles on intestinal microbiota and gut-associated immune responses in the ileum of Sprague-Dawley rats. Nanotoxicology *9*, 279–289.

Wise, J.P., Goodale, B.C., Wise, S.S., Craig, G.A., Pongan, A.F., Walter, R.B., Thompson, W.D., Ng, A.-K., Aboueissa, A.-M., and Mitani, H. (2010). Silver nanospheres are cytotoxic and genotoxic to fish cells. Aquat. Toxicol. *97*, 34–41.

Zaki, M.H., Man, S.M., Vogel, P., Lamkanfi, M., and Kanneganti, T.-D. (2014). Salmonella exploits NLRP12-dependent innate immune signaling to suppress host defenses during infection. Proc. Natl. Acad. Sci. *111*, 385–390.

Zänker, H., and Schierz, A. (2012). Engineered Nanoparticles and Their Identification Among Natural Nanoparticles. Annu. Rev. Anal. Chem. *5*, 107–132.

Zhang, Y., Ding, Z., Zhao, G., Zhang, T., Xu, Q., Cui, B., and Liu, J.-X. (2018). Transcriptional responses and mechanisms of copper nanoparticle toxicology on zebrafish embryos. J. Hazard. Mater. *344*, 1057–1068.

Graphical abstract. European eels were exposed to food-borne gold nanoparticles. The whole transcriptome response was assessed by RNA-sequencing in their brain and their liver.
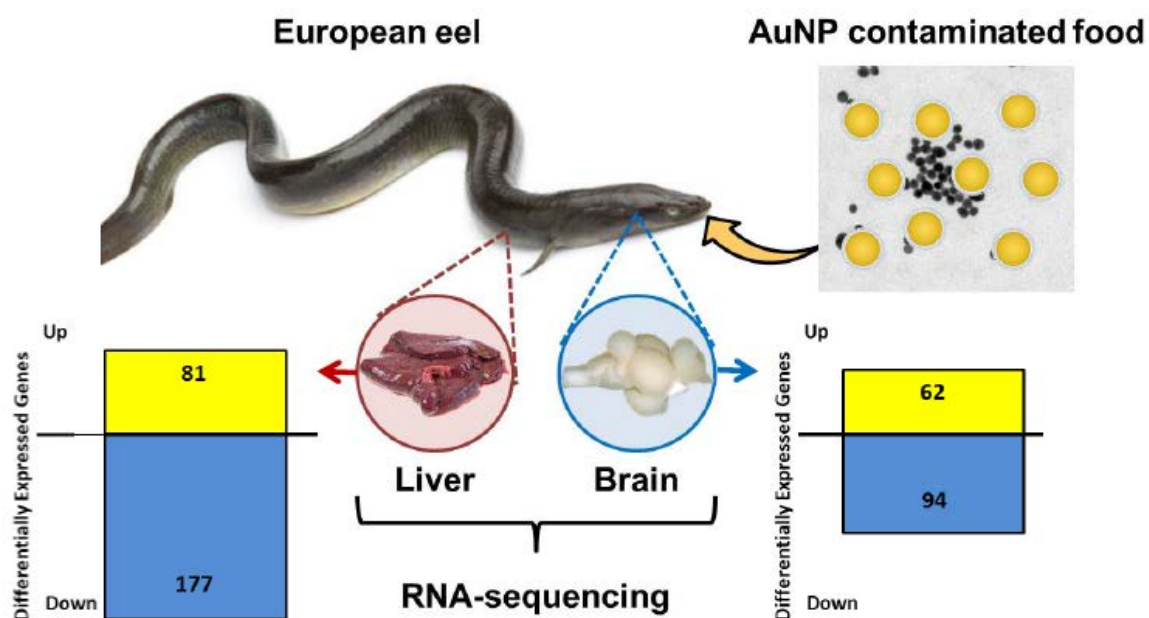
Figure 1. TEM micrograph of gold nanoparticles prior to incorporation into fish food

(after Brisson and Mornet, 2009).
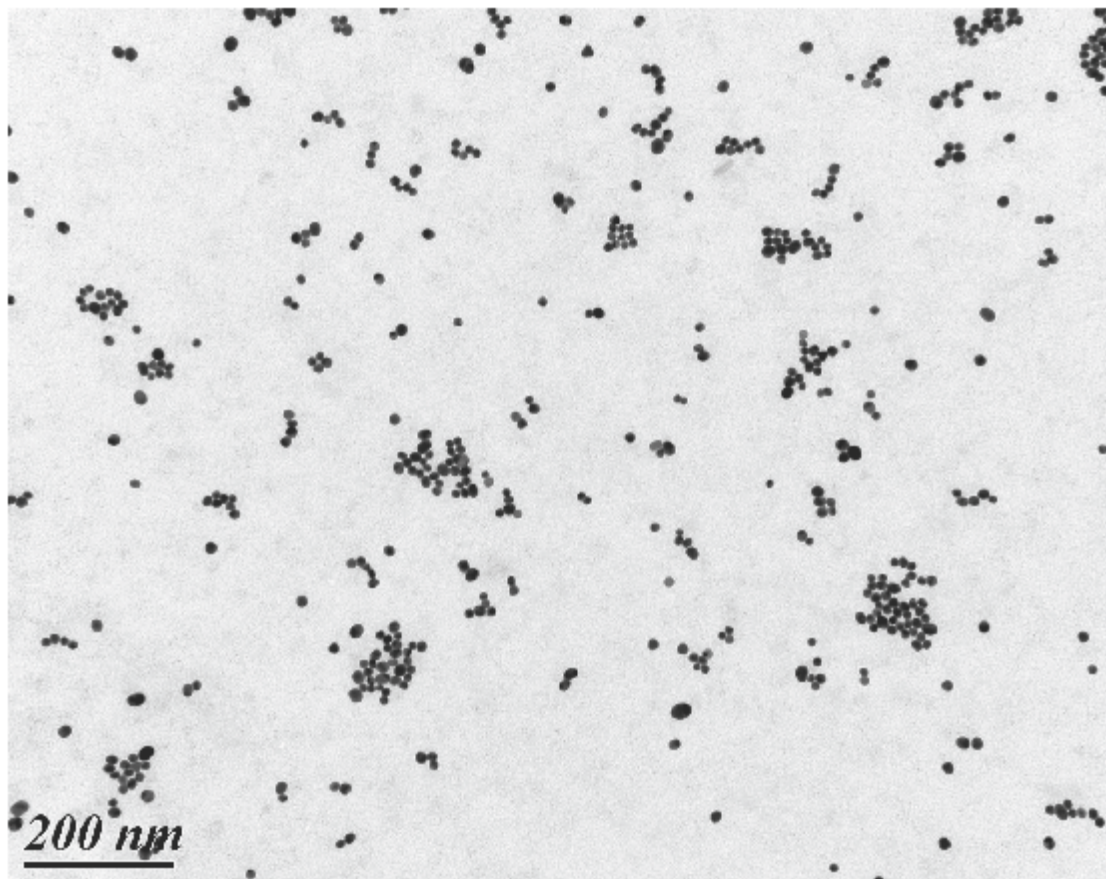
Figure 1. TEM micrograph of gold nanoparticles prior to incorporation into fish food (after Brisson and Mornet, 2009).

Figure 2. Gold accumulation in the intestine, kidney and liver of eels after a 21-day AuNP trophic exposure in NP0 and NP1 conditions (mean ± SE, $n = 6$). Values were compared by a Kruskall-Wallis procedure. The symbol * indicates a significant difference ($p<0.05$).
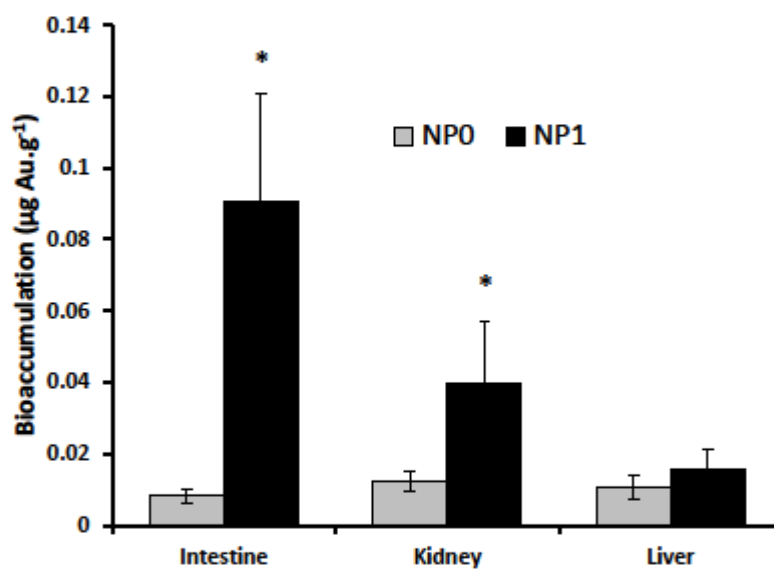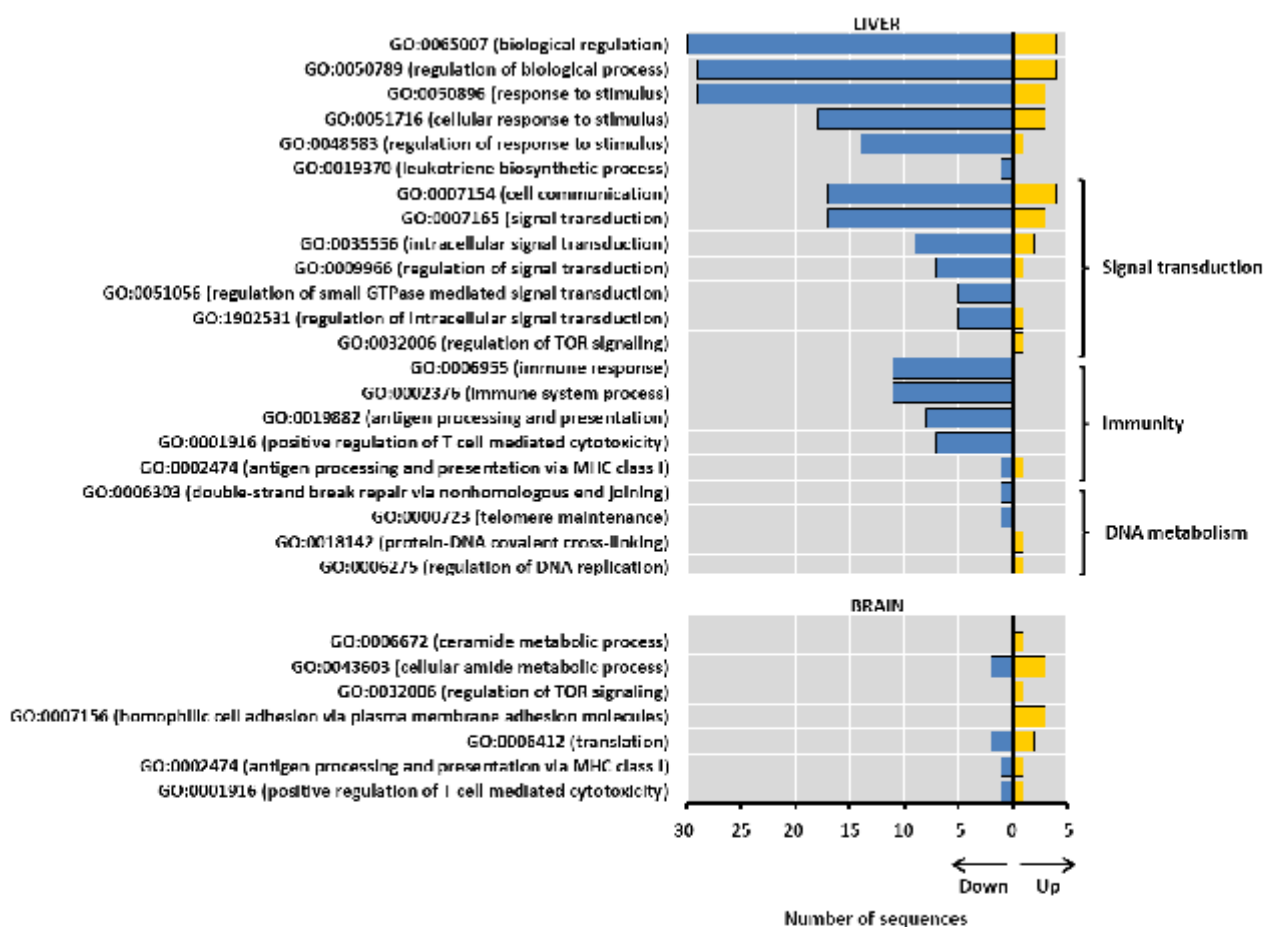

Figure 2. Gold accumulation in the intestine, kidney and liver of eels after a 21-day AuNP trophic exposure in NP0 and NP1 conditions (mean ± SE, $n = 6$). Values were compared by a Kruskall-Wallis procedure. The symbol * indicates a significant difference ($p<0.05$).

Figure 3. Number of genes differentially expressed in the liver and brain of NP1 eels after 21 days of exposure. Up- and Down-regulated genes are indicated in yellow and blue, respectively.
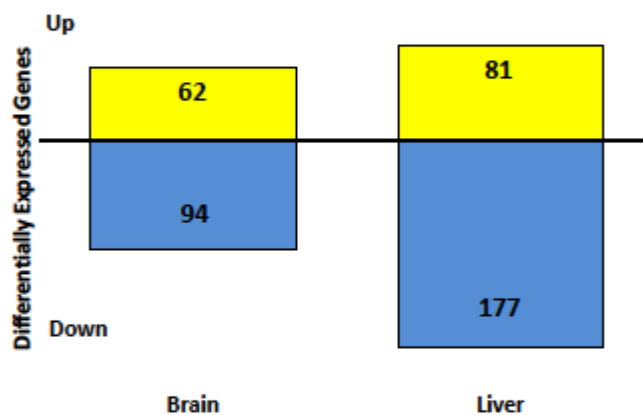
Figure 3. Number of genes differentially expressed in the liver and brain of NP1 eels after 21 days of exposure. Up- and Down-regulated genes are indicated in yellow and blue, respectively.

Figure 4. Gene Ontology (GO) analysis regarding the biological processes affected in the brain (lower panel) and liver (upper panel) of eels fed with AuNP-enriched food at 1 mg Au.kg^{-1} (fw) during 21 days. X-axis: Distribution between numbers of sequences up-(yellow) and down-regulated (blue) are for NP1 eels compared to controls.

Figure 4. Gene Ontology (GO) analysis regarding the biological processes affected in the brain (lower panel) and liver (uppe panel) of eels fed with AuNP-enriched food at 1 mg Au.kg^{-1} (fw) during 21 days. Distribution between numbers of sequences and down-regulated (x-axis) are for NP1 eels compared to controls.

Table 1. Biometry, food consumption and various condition indices of eels after 21 days (mean $\pm$ SE, $n =$ 6)

	NP0	NP1	NP10
Length (cm)	33.78 ± 0.56	33.63 ± 0.58	33.98 ± 0.68
Weight t_0 (g)	56.83 ± 3.75	57.5 ± 3.10	64.33 ± 3.56
Food consumed (%)	100 ± 0 (a)	93.65 ± 2.17 (a)	56.49 ± 19.01 (b)
Weight t_{21} (g)	71.00 ± 4.80 (ab)	63.83 ± 2.46 (b)	77.33 ± 3.84 (a)
Weight gain (g/g food)	0.43 ± 0.07	0.21 ± 0.13	1.01 ± 0.24
K	0.18 ± 0.01	0.17 ± 0.01	0.20 ± 0.01
ISI	0.71 ± 0.06 (a)	0.43 ± 0.09 (b)	0.21 ± 0.03 (c)
HSI	1.33 ± 0.10	1.36 ± 0.11	1.10 ± 0.09
SSI	0.13 ± 0.02 (a)	0.08 ± 0.01 (b)	0.09 ± 0.01 (ab)

NP0, NP1 and NP10 = food contaminated with 0, 1 and 10 mg of AuNP per kg, respectively.
K = Fulton index; ISI = Intestine Somatic Index; HSI = Hepato-Somatic Index; SSI = Spleen Somatic Index.
Letters between brackets indicate significant differences amongst groups (p<0.05)

Table 2. List of DEGs[a] involved in immunity and signal transduction

	Gene ID	FC liver	FC brain	Description
Immunity	CitLOC106588401.14.16	0.24		class I histocompatibility antigen, F10 alpha chain-like [Salmo salar]
	CitLOC105010185.2.4	0.26	0.49	major histocompatibility complex class I-related gene protein-like [Esox lucius]
	Citcontig_04334	0.31		major histocompatibility complex class II [Lepisosteus oculatus]
	CitLOC106588401.3.16	0.32		class I histocompatibility antigen, F10 alpha chain-like [Salmo salar]
	CitLOC106588401.1.16	0.33		class I histocompatibility antigen, F10 alpha chain-like [Salmo salar]
	CitLOC107746875	0.35		C-X-C motif chemokine 10-like [Sinocyclocheilus rhinocerous]
	CitLOC106606884	0.36		perforin-1-like [Salmo salar]
	CitLOC107563205	0.36		class I histocompatibility antigen [Sinocyclocheilus grahami]
	CitLOC107719853.5.5	0.37		H-2 class I histocompatibility antigen, Q10 alpha chain-like [Sinocyclocheilus rhinocerous]
	Citcontig_23527	0.39		C-X-C motif chemokine 11-6-like [Scleropages formosus]

Gene ID	Value	Avg	Description
CitLOC107719853.2.5	0.39		H-2 class I histocompatibility antigen, Q10 alpha chain-like [Sinocyclocheilus rhinocerous]
CitLOC106569935.6.10	1.71	1.81	major histocompatibility complex class I-related gene protein-like [Salmo salar]

Signal transduction			
Citcd3z.2.2	0.28		CD3zeta-2 precursor [Salmo salar]
Citcd3z.1.2	0.37		CD3zeta-2 precursor [Salmo salar]
Citcontig_00766	0.39		Predicted protein [Lepisosteus oculatus]
Citrgs18	0.42		regulator of G-protein signaling 18 [Esox lucius]
CitLOC106608770	0.44		active breakpoint cluster region-related protein-like [Salmo salar]
CitLOC106585107.2.2	0.44		rho GTPase-activating protein 25-like [Salmo salar]
CitLOC107758237	0.47		RAS guanyl-releasing protein 1-like [Sinocyclocheilus rhinocerous]
CitLOC103044816	0.48		probable G-protein coupled receptor 34 [Astyanax mexicanus]
Citdgkk.2.2	0.49		diacylglycerol kinase kappa [Lepisosteus oculatus]
Citvav1	0.51		proto-oncogene vav [Lepisosteus oculatus]
Citplek	0.51		pleckstrin [Lepisosteus oculatus]
Citjak3	0.52		tyrosine-protein kinase JAK3 [Lepisosteus oculatus]
CitLOC103039110.3.5	0.52		regulator of G-protein signaling 3-like [Astyanax mexicanus]
CitLOC106580794	0.53		rap1 GTPase-activating protein 2-like [Salmo salar]
Citcontig_14893	0.54		SH2 domain-containing protein 3C-like [Pygocentrus nattereri]
Citrasgrp2.2.2	0.57		RAS guanyl-releasing protein 2 [Pundamilia nyererei]
CitLOC106571892	0.58		FYVE, RhoGEF and PH domain-containing protein 3-like [Salmo salar]
CitWSB1.3.5	1.65		WD repeat and SOCS box-containing protein 1 [Danio rerio]
Citlamtor3.3.4	2.19	2.29	ragulator complex protein LAMTOR3 [Esox lucius]
Cititgb4	2.22		integrin beta-4 [Lepisosteus oculatus]
CitLOC107668371	2.57		ras-associated and pleckstrin homology domains-containing protein 1-like [Sinocyclocheilus anshuiensis]

ᵃ (False Discovery Rate ≤ 0.05)

DEG: Differentially expressed

Table 3. Differentially expressed genes that were commonly affected in the liver and brain of eels fed with AuNP-enriched food at 1 mg Au.kg^{-1} during 21 days

Protein Name	Function/ Involvement	Contig ID	Liver		Brain	
			FC	FDR	FC	FDR
No Hit	Unknown	Citcontig_00047	2.52	0.43×10^{-2}	1.89	0.46×10^{-2}
No Hit	Unknown	Citcontig_05910	0.22	0.24×10^{-5}	0.59	0.19×10^{-2}
No Hit	Unknown	Citcontig_16608	2.88	0.01	1.88	0.03
gstk1	Oxidation-reduction process	Citgstk1.2.3	0.52	0.02	-	n.s
		Citgstk1.3.3	-	n.s	0.60	0.04
lamtor3	Regulation of late endosomal traffic and cell proliferation	Citlamtor3.3.4	2.19	0.01	2.29	0.12×10^{-3}
scya112	chemokine	CitLOC100304631	3.79	0.73×10^{-4}	1.92	0.03
mr1	Innate immunity	CitLOC105010185.2.4	0.26	0.37×10^{-3}	0.49	0.84×10^{-2}
napb	Transport	CitLOC102683706.4.4	0.36	0.11×10^{-2}	0.46	0.21×10^{-2}
nlrc3	Innate immunity, inflammasome	CitLOC105006816.3.3	1.89	0.01	-	n.s
		CitLOC106579984.5.5	-	n.s	1.73	0.04
nlrp12	Inflammasome	CitLOC106573426.1.4	1.98	0.03	-	n.s
		CitLOC10659231 3.10.10	-	n.s	1.72	0.04
per3	Biological rhythms	Citper3.3.5	0.51	0.04	0.50	0.34×10^{-4}
sptbn1	Cytoskeleton movement (calcium-dependent)	CitLOC103353295.2.2	1.94	0.33×10^{-2}	1.71	0.44×10^{-2}
tnrc6b	RNA-mediated gene silencing	CitLOC107731400.2.3	1.74	0.03	-	n.s
		CitLOC106589538	-	n.s	0.61	0.04

FC = Fold Change comapred to NP0 condition; n.s = non-significant;
FDR = False Discovery Rate.